



# Vertex Approximate Gradient Scheme for Hybrid Dimensional Two-Phase Darcy Flows in Fractured Porous Media

Konstantin Brenner, Mayya Groza, Cindy Guichard, Roland Masson

► **To cite this version:**

Konstantin Brenner, Mayya Groza, Cindy Guichard, Roland Masson. Vertex Approximate Gradient Scheme for Hybrid Dimensional Two-Phase Darcy Flows in Fractured Porous Media . The International Symposium of Finite Volumes for Complex Applications VII, Jun 2014, Berlin, Germany. 2014, Finite Volumes for Complex Applications VII- Elliptic, Parabolic and Hyperbolic Problems. <hal-01313353>

**HAL Id: hal-01313353**

**<https://hal.archives-ouvertes.fr/hal-01313353>**

Submitted on 9 May 2016

**HAL** is a multi-disciplinary open access archive for the deposit and dissemination of scientific research documents, whether they are published or not. The documents may come from teaching and research institutions in France or abroad, or from public or private research centers.

L'archive ouverte pluridisciplinaire **HAL**, est destinée au dépôt et à la diffusion de documents scientifiques de niveau recherche, publiés ou non, émanant des établissements d'enseignement et de recherche français ou étrangers, des laboratoires publics ou privés.



# Vertex Approximate Gradient Scheme for Hybrid Dimensional Two-Phase Darcy Flows in Fractured Porous Media

K. Brenner, M. Groza, C. Guichard, R. Masson

**Abstract** This paper presents the Vertex Approximate Gradient (VAG) discretization of a two-phase Darcy flow in discrete fracture networks (DFN) taking into account the mass exchange between the matrix and the fracture. We consider the asymptotic model for which the fractures are represented as interfaces of codimension one immersed in the matrix domain with continuous pressures at the matrix fracture interface. Compared with Control Volume Finite Element (CVFE) approaches, the VAG scheme has the advantage to avoid the mixing of the fracture and matrix rocktypes at the interfaces between the matrix and the fractures, while keeping the low cost of a nodal discretization on unstructured meshes. The convergence of the scheme is proved under the assumption that the relative permeabilities are bounded from below by a strictly positive constant but cover the case of discontinuous capillary pressures. The efficiency of our approach compared with CVFE discretizations is shown on a 3D fracture network with very low matrix permeability.

---

K. Brenner

University Nice Sophia Antipolis, and team COFFEE, INRIA Sophia Antipolis Méditerranée, France, e-mail: konstantin.brenner@unice.fr

M. Groza

University Nice Sophia Antipolis, and team COFFEE, INRIA Sophia Antipolis Méditerranée, France, e-mail: mayya.groza@unice.fr

C. Guichard

Sorbonne Universités, UPMC Univ Paris 06, UMR 7598, Laboratoire Jacques-Louis Lions, F-75005, Paris, France, e-mail: guichard@ljl.math.upmc.fr

R. Masson

University Nice Sophia Antipolis, and team COFFEE, INRIA Sophia Antipolis Méditerranée, France, e-mail: roland.masson@unice.fr

## 1 Hybrid dimensional Two-Phase Darcy Flow Model in Fractured Porous Media

Let  $\Omega$  denotes a bounded polyhedral domain of  $\mathbb{R}^d$ ,  $d = 2, 3$ . We consider the asymptotic model introduced in [1] where fractures are represented as interfaces of codimension 1. Let  $\bar{\Gamma} = \bigcup_{i \in I} \bar{\Gamma}_i$  denotes the network of fractures  $\Gamma_i \subset \Omega$ ,  $i \in I$ , such that each  $\Gamma_i$  is a planar polygonal simply connected domain. It is assumed that the angles of  $\Gamma_i$  are strictly lower than  $2\pi$  and that  $\Gamma_i \cap \Gamma_j = \emptyset$  for all  $i \neq j$ . It is also assumed that  $\Sigma_{i,0} = \bar{\Gamma}_i \cap \partial\Omega$  has a vanishing  $d-1$  measure. We will denote by  $d\tau(\mathbf{x})$  the  $d-1$  dimensional Lebesgue measure on  $\Gamma$ . Let  $H^1(\Gamma)$  denote the set of functions  $v = (v_i)_{i \in I}$  such that  $v_i \in H^1(\Gamma_i)$ ,  $i \in I$  with continuous traces at the fracture intersections, and endowed with the norm  $\|v\|_{H^1(\Gamma)}^2 = \sum_{i \in I} \|v_i\|_{H^1(\Gamma_i)}^2$ . Its subspace with vanishing traces on  $\Sigma_0 = \bigcup_{i \in I} \Sigma_{i,0}$  is denoted by  $H_{\Sigma_0}^1(\Gamma)$ . The gradient operator from  $H^1(\Omega)$  to  $L^2(\Omega)^d$  is denoted by  $\nabla$ , and the tangential gradient from  $H^1(\Gamma)$  to  $L^2(\Gamma)^{d-1}$  by  $\nabla_\tau$ . Let us also consider the trace operator  $\gamma$  from  $H^1(\Omega)$  to  $L^2(\Gamma)$ . We can now define the hybrid dimensional function spaces that will be used in the variational formulation of the two-phase Darcy flow model:

$$V = \{v \in H^1(\Omega), \gamma v \in H^1(\Gamma)\}, \text{ and its subspace } V_0 = \{v \in H_0^1(\Omega), \gamma v \in H_{\Sigma_0}^1(\Gamma)\}.$$

The space  $V_0$  is endowed with the norm  $\|v\|_V^2 = \|\nabla v\|_{L^2(\Omega)^d}^2 + \|\nabla_\tau \gamma v\|_{L^2(\Gamma)^{d-1}}^2$ .

Let  $u^2$  (resp.  $u^1$ ) denote the wetting (resp. non wetting) phase pressure,  $p = u^1 - u^2$  the capillary pressure, and  $p_{\text{ini}} \in V$  the initial capillary pressure distribution. For the sake of simplicity in the convergence analysis, homogeneous Dirichlet boundary conditions are assumed for  $u^1$  and  $u^2$  at the boundary  $\partial\Omega$ , as well as at  $\Sigma_0$  for  $\gamma u^1$  and  $\gamma u^2$ . Let us denote by  $S_m^1(\mathbf{x}, p)$  (resp.  $S_f^1(\mathbf{x}, p)$ ) the inverses of the monotone graph extension of the capillary pressure curves in the matrix domain  $\Omega$  (resp. in the fracture network  $\Gamma$ ), and let us set  $S_m^2 = 1 - S_m^1$  (resp.  $S_f^2 = 1 - S_f^1$ ). In the matrix domain  $\Omega$  (resp. in the fracture network  $\Gamma$ ), let us denote by  $k_m^\alpha(\mathbf{x}, S_m^\alpha)$  (resp.  $k_f^\alpha(\mathbf{x}, S_f^\alpha)$ ),  $\alpha \in \{1, 2\}$ , the phase mobilities, by  $\phi_m(\mathbf{x})$  (resp.  $\phi_f(\mathbf{x})$ ) the porosity, and by  $\Lambda_m(\mathbf{x})$  (resp.  $\Lambda_f(\mathbf{x})$ ) the permeability tensor. We also denote by  $d_f(\mathbf{x})$ ,  $\mathbf{x} \in \Gamma$  the width of the fractures, and by  $d\tau_f(\mathbf{x}) = d_f(\mathbf{x})d\tau(\mathbf{x})$  the weighted Lebesgue  $d-1$  dimensional measure on  $\Gamma$  defined by  $d\tau_f(\mathbf{x}) = d_f(\mathbf{x})d\tau(\mathbf{x})$ . The hybrid dimensional phase pressures weak formulation amounts to find  $u^1, u^2 \in L^2(0, T; V_0)$  satisfying the following variational equalities for  $\alpha \in \{1, 2\}$ , and for all  $\varphi \in C_c^\infty([0, T] \times \Omega)$ :

$$\left\{ \begin{array}{l} \int_0^T \int_{\Omega} \left( -\phi_m(\mathbf{x}) S_m^\alpha(\mathbf{x}, p) \partial_t \varphi(\mathbf{x}, t) + k_m^\alpha(\mathbf{x}, S_m^\alpha(\mathbf{x}, p)) \Lambda_m(\mathbf{x}) \nabla u^\alpha(\mathbf{x}, t) \cdot \nabla \varphi(\mathbf{x}, t) \right) d\mathbf{x} dt \\ + \int_0^T \int_{\Gamma} -\phi_f(\mathbf{x}) S_f^\alpha(\mathbf{x}, \gamma p) \partial_t \gamma \varphi(\mathbf{x}, t) d\tau_f(\mathbf{x}) dt \\ + \int_0^T \int_{\Gamma} k_f^\alpha(\mathbf{x}, S_f^\alpha(\mathbf{x}, \gamma p)) \Lambda_f(\mathbf{x}) \nabla_\tau \gamma u^\alpha(\mathbf{x}, t) \cdot \nabla_\tau \gamma \varphi(\mathbf{x}, t) d\tau_f(\mathbf{x}) dt \\ + \int_{\Omega} \phi_m(\mathbf{x}) S_m^\alpha(\mathbf{x}, p_{\text{ini}}) \varphi(\mathbf{x}, 0) d\mathbf{x} dt + \int_{\Gamma} \phi_f(\mathbf{x}) S_f^\alpha(\mathbf{x}, \gamma p_{\text{ini}}) \varphi(\mathbf{x}, 0) d\tau_f(\mathbf{x}) dt \\ - \int_0^T \int_{\Omega} h_m^\alpha(\mathbf{x}, t) \varphi(\mathbf{x}, t) d\mathbf{x} dt - \int_0^T \int_{\Gamma} h_f^\alpha(\mathbf{x}, t) \gamma \varphi(\mathbf{x}, t) d\tau_f(\mathbf{x}) dt = 0, \end{array} \right. \quad (1)$$

where the function  $h_m^\alpha$  (resp.  $h_f^\alpha$ ),  $\alpha \in \{1, 2\}$  stands for the source term in the matrix domain  $\Omega$  (resp. in the fracture network  $\Gamma$ ).

## 2 Vertex Approximate Gradient Discretization

In the spirit of [3], we consider generalised polyhedral meshes of  $\Omega$ . Let  $\mathcal{M}$  be the set of cells that are disjoint open polyhedral subsets of  $\Omega$  such that  $\bigcup_{K \in \mathcal{M}} \bar{K} = \bar{\Omega}$ . For all  $K \in \mathcal{M}$ ,  $\mathbf{x}_K$  denotes the so-called ‘‘centre’’ of the cell  $K$  under the assumption that  $K$  is star-shaped with respect to  $\mathbf{x}_K$ . We then denote by  $\mathcal{F}_K$  the set of interfaces of non zero  $d - 1$  dimensional measure among the interior faces  $\bar{K} \cap \bar{L}$ ,  $L \in \mathcal{M}$ , and the boundary interface  $\bar{K} \cap \partial\Omega$ , which possibly splits in several boundary faces. Let us denote by  $\mathcal{F} = \bigcup_{K \in \mathcal{M}} \mathcal{F}_K$  the set of all faces of the mesh. Remark that the faces are not assumed to be planar, hence the term ‘‘generalised polyhedral mesh’’. For  $\sigma \in \mathcal{F}$ , let  $\mathcal{E}_\sigma$  be the set of interfaces of non zero  $d - 2$  dimensional measure among the interfaces  $\sigma \cap \sigma'$ ,  $\sigma' \in \mathcal{F}$ . Then, we denote by  $\mathcal{E} = \bigcup_{\sigma \in \mathcal{F}} \mathcal{E}_\sigma$  the set of all edges of the mesh. Let  $\mathcal{V}_\sigma = \bigcup_{e, e' \in \mathcal{E}_\sigma, e \neq e'} (e \cap e')$  be the set of vertices of  $\sigma$ , for each  $K \in \mathcal{M}$  we define  $\mathcal{V}_K = \bigcup_{\sigma \in \mathcal{F}_K} \mathcal{V}_\sigma$ , and we also denote by  $\mathcal{V} = \bigcup_{K \in \mathcal{M}} \mathcal{V}_K$  the set of all vertices of the mesh. It is then assumed that for each face  $\sigma \in \mathcal{F}$ , there exists a so-called ‘‘centre’’ of the face  $\mathbf{x}_\sigma \in \sigma \setminus \bigcup_{e \in \mathcal{E}_\sigma} e$  such that  $\mathbf{x}_\sigma = \sum_{\mathbf{s} \in \mathcal{V}_\sigma} \beta_{\sigma, \mathbf{s}} \mathbf{x}_\mathbf{s}$ , with  $\sum_{\mathbf{s} \in \mathcal{V}_\sigma} \beta_{\sigma, \mathbf{s}} = 1$ , and  $\beta_{\sigma, \mathbf{s}} \geq 0$  for all  $\mathbf{s} \in \mathcal{V}_\sigma$ ; moreover the face  $\sigma$  is assumed to match with the union of the triangles  $T_{\sigma, e}$  defined by the face centre  $\mathbf{x}_\sigma$  and each edge  $e \in \mathcal{E}_\sigma$ . The mesh is also supposed to be conforming w.r.t. the fracture network  $\Gamma$  in the sense that for all  $i \in I$  there exist the subsets  $\mathcal{F}_{\Gamma_i}$  of  $\mathcal{F}$  such that  $\bar{\Gamma}_i = \bigcup_{\sigma \in \mathcal{F}_{\Gamma_i}} \bar{\sigma}$ . We will denote by  $\mathcal{F}_\Gamma$  the set of fracture faces  $\bigcup_{i \in I} \mathcal{F}_{\Gamma_i}$ . This geometrical discretization of  $\Omega$  and  $\Gamma$  is denoted in the following by  $\mathcal{D}$ .

The VAG discretization has been introduced in [3] for diffusive problems on heterogeneous anisotropic media. Its extension to the hybrid dimensional Darcy model is based on the following vector space of degrees of freedom:

$$X_{\mathcal{D}} = \{v_K, v_{\mathbf{s}}, v_\sigma \in \mathbb{R}, K \in \mathcal{M}, \mathbf{s} \in \mathcal{V}, \sigma \in \mathcal{F}_\Gamma\},$$

and its subspace with homogeneous Dirichlet boundary conditions on  $\partial\Omega$ :

$$X_{\mathcal{D}}^0 = \{v \in X_{\mathcal{D}} \mid v_{\mathbf{s}} = 0 \text{ for } \mathbf{s} \in \mathcal{V}_{ext}\}.$$

where  $\mathcal{V}_{ext} = \mathcal{V} \cap \partial\Omega$  denotes the set of boundary vertices, and  $\mathcal{V}_{int} = \mathcal{V} \setminus \partial\Omega$  denotes the set of interior vertices.

A finite element discretization of  $V$  is built using a tetrahedral sub-mesh of  $\mathcal{M}$  and a second order interpolation at the face centres  $\mathbf{x}_{\sigma}$ ,  $\sigma \in \mathcal{F} \setminus \mathcal{F}_{\Gamma}$  defined by the operator  $I_{\sigma} : X_{\mathcal{D}} \rightarrow \mathbb{R}$  such that  $I_{\sigma}(v) = \sum_{\mathbf{s} \in \mathcal{V}_{\sigma}} \beta_{\sigma, \mathbf{s}} v_{\mathbf{s}}$ . The tetrahedral sub-mesh is defined by  $\mathcal{T} = \{T_{K, \sigma, e}, e \in \mathcal{E}_{\sigma}, \sigma \in \mathcal{F}_K, K \in \mathcal{M}\}$  where  $T_{K, \sigma, e}$  is the tetrahedron joining the cell centre  $\mathbf{x}_K$  to the triangle  $T_{\sigma, e}$ .

For a given  $v \in X_{\mathcal{D}}$ , we define the function  $\pi_{\mathcal{T}} v \in V$  as the continuous piecewise affine function on each tetrahedron of  $\mathcal{T}$  such that  $\pi_{\mathcal{T}} v(\mathbf{x}_K) = v_K$ ,  $\pi_{\mathcal{T}} v(\mathbf{s}) = v_{\mathbf{s}}$ ,  $\pi_{\mathcal{T}} v(\mathbf{x}_{\sigma}) = v_{\sigma}$ , and  $\pi_{\mathcal{T}} v(\mathbf{x}_{\sigma'}) = I_{\sigma'}(v)$  for all  $K \in \mathcal{M}$ ,  $\mathbf{s} \in \mathcal{V}$ ,  $\sigma \in \mathcal{F}_{\Gamma}$ , and  $\sigma' \in \mathcal{F} \setminus \mathcal{F}_{\Gamma}$ . Discrete gradient operators are defined this from finite element discretization of  $V$  by

$$\nabla_{\mathcal{D}_m} : X_{\mathcal{D}} \rightarrow L^2(\Omega)^d \text{ such that } \nabla_{\mathcal{D}_m} v = \nabla \pi_{\mathcal{T}} v,$$

in the matrix, and by

$$\nabla_{\mathcal{D}_f} : X_{\mathcal{D}} \rightarrow L^2(\Gamma)^{d-1} \text{ such that } \nabla_{\mathcal{D}_f} v = \nabla_{\tau} \gamma \pi_{\mathcal{T}} v,$$

in the fracture network. In addition, the VAG discretization uses two non conforming piecewise constant reconstructions of functions from  $X_{\mathcal{D}}$  into respectively  $L^2(\Omega)$  and  $L^2(\Gamma)$  based on partitions of each cell and of each fracture face denoted by  $K = \omega_K \cup \left( \bigcup_{\mathbf{s} \in \mathcal{V}_K \cap \mathcal{V}_{int}} \omega_{K, \mathbf{s}} \right) \cup \left( \bigcup_{\sigma \in \mathcal{F}_K \cap \mathcal{F}_{\Gamma}} \omega_{K, \sigma} \right)$ , for all  $K \in \mathcal{M}$ , and by  $\sigma = \Sigma_{\sigma} \cup \left( \bigcup_{\mathbf{s} \in \mathcal{V}_{\sigma} \cap \mathcal{V}_{int}} \Sigma_{\sigma, \mathbf{s}} \right)$  for all  $\sigma \in \mathcal{F}_{\Gamma}$ . Then, the function reconstruction operators are defined by  $\pi_{\mathcal{D}_m} v(\mathbf{x}) = \begin{cases} v_K & \text{for all } \mathbf{x} \in \omega_K, K \in \mathcal{M}, \\ v_{\mathbf{s}} & \text{for all } \mathbf{x} \in \omega_{K, \mathbf{s}}, \mathbf{s} \in \mathcal{V}_K \cap \mathcal{V}_{int}, K \in \mathcal{M}, \\ v_{\sigma} & \text{for all } \mathbf{x} \in \omega_{K, \sigma}, \sigma \in \mathcal{F}_K \cap \mathcal{F}_{\Gamma}, K \in \mathcal{M}, \end{cases}$

and  $\pi_{\mathcal{D}_f} v(\mathbf{x}) = \begin{cases} v_{\sigma} & \text{for all } \mathbf{x} \in \Sigma_{\sigma}, \sigma \in \mathcal{F}_{\Gamma}, \\ v_{\mathbf{s}} & \text{for all } \mathbf{x} \in \Sigma_{\sigma, \mathbf{s}}, \mathbf{s} \in \mathcal{V}_{\sigma} \cap \mathcal{V}_{int}, \sigma \in \mathcal{F}_{\Gamma}. \end{cases}$

It is important to notice that, in the practical case when the space discretization is conforming with respect to the heterogeneities and when the source term  $h_m^{\alpha}$  (resp.  $h_f^{\alpha}$ ) is a cellwise (resp. facewise) constant function, the implementation of the VAG scheme does not require to build these partitions. In that case, it is sufficient to define the matrix volume fractions  $\alpha_{K, \mathbf{s}} = \frac{\int_{\omega_{K, \mathbf{s}}} dx}{\int_K dx}$ ,  $\mathbf{s} \in \mathcal{V}_K \cap \mathcal{V}_{int}$ ,  $K \in \mathcal{M}$ ,  $\alpha_{K, \sigma} = \frac{\int_{\omega_{K, \sigma}} dx}{\int_K dx}$ ,  $\sigma \in \mathcal{F}_K \cap \mathcal{F}_{\Gamma}$ ,  $K \in \mathcal{M}$ , constrained to satisfy  $\alpha_{K, \mathbf{s}} \geq 0$ ,  $\alpha_{K, \sigma} \geq 0$ , and  $\sum_{\mathbf{s} \in \mathcal{V}_K \cap \mathcal{V}_{int}} \alpha_{K, \mathbf{s}} + \sum_{\sigma \in \mathcal{F}_K \cap \mathcal{F}_{\Gamma}} \alpha_{K, \sigma} \leq 1$ , as well as the fracture volume fractions  $\alpha_{\sigma, \mathbf{s}} = \frac{\int_{\Sigma_{\sigma, \mathbf{s}}} d\tau_f(\mathbf{x})}{\int_{\Sigma_{\sigma}} d\tau_f(\mathbf{x})}$ ,  $\mathbf{s} \in \mathcal{V}_{\sigma} \cap \mathcal{V}_{int}$ ,  $\sigma \in \mathcal{F}_{\Gamma}$ , constrained to satisfy  $\alpha_{\sigma, \mathbf{s}} \geq 0$ , and  $\sum_{\mathbf{s} \in \mathcal{V}_{\sigma} \cap \mathcal{V}_{int}} \alpha_{\sigma, \mathbf{s}} \leq 1$ . The convergence of the scheme will be shown to hold whatever the choice of these volume fractions. As will be detailed in the numerical section, this flexibility is a crucial asset, compared with usual CVFE approaches [6], [5], in order to improve the accuracy of the scheme for highly heterogeneous test cases.

For  $N \in \mathbb{N}^*$ , let us consider generally nonuniform discretization  $t^0 = 0 < t^1 < \dots < t^{n-1} < t^n \dots < t^N = T$  of the time interval  $[0, T]$ . We denote the time steps by  $\Delta t^n = t^n - t^{n-1}$  for all  $n \in \{1, \dots, N\}$  while  $\Delta t$  stands for the whole sequence  $(\Delta t^n)_{n \in \{1, \dots, N\}}$ . Let us denote by  $u^{\alpha, n} \in X_{\mathcal{D}}^0$ ,  $\alpha \in \{1, 2\}$  the discrete phase pressures, and by  $p^n = u^{1, n} - u^{2, n}$  the discrete capillary pressure at time  $t^n$  for all  $n \in \{1, \dots, N\}$ . Given an approximation  $p^0 \in X_{\mathcal{D}}$  of the initial capillary pressure  $p_{\text{ini}}$ , the VAG discretization of the two-phase Darcy flow model in phase pressures formulation (1) looks for  $u^\alpha = \left( u^{\alpha, n} \in X_{\mathcal{D}}^0 \right)_{n \in \{1, \dots, N\}}$ ,  $\alpha \in \{1, 2\}$ , such that for  $\alpha \in \{1, 2\}$ , and for all  $v \in X_{\mathcal{D}}^0$  one has

$$\begin{cases} \int_{\Omega} \phi_m \frac{S_{\mathcal{D}_m}^{\alpha, n} - S_{\mathcal{D}_m}^{\alpha, n-1}}{\Delta t^n} \pi_{\mathcal{D}_m} v \, d\mathbf{x} + \int_{\Omega} k_{\mathcal{D}_m}^{\alpha, n} \Lambda_m \nabla_{\mathcal{D}_m} u^{\alpha, n} \cdot \nabla_{\mathcal{D}_m} v \, d\mathbf{x} \\ + \int_{\Gamma} \phi_f \frac{S_{\mathcal{D}_f}^{\alpha, n} - S_{\mathcal{D}_f}^{\alpha, n-1}}{\Delta t^n} \pi_{\mathcal{D}_f} v \, d\tau_f(\mathbf{x}) + \int_{\Gamma} k_{\mathcal{D}_f}^{\alpha, n} \Lambda_f \nabla_{\mathcal{D}_f} u^{\alpha, n} \cdot \nabla_{\mathcal{D}_f} v \, d\tau_f(\mathbf{x}) \\ = \frac{1}{\Delta t^n} \int_{t^{n-1}}^{t^n} \left( \int_{\Omega} h_m^\alpha \pi_{\mathcal{D}_m} v \, d\mathbf{x} + \int_{\Gamma} h_f^\alpha \pi_{\mathcal{D}_f} v \, d\tau_f(\mathbf{x}) \right) dt, \end{cases} \quad (2)$$

where  $S_{\mathcal{D}_m}^{\alpha, n}(\mathbf{x}) = S_m^\alpha(\mathbf{x}, \pi_{\mathcal{D}_m} p^n(\mathbf{x}))$ ,  $S_{\mathcal{D}_f}^{\alpha, n}(\mathbf{x}) = S_f^\alpha(\mathbf{x}, \pi_{\mathcal{D}_f} p^n(\mathbf{x}))$ , and  $k_{\mathcal{D}_m}^{\alpha, n}(\mathbf{x}) = k_m^\alpha(\mathbf{x}, S_{\mathcal{D}_m}^{\alpha, n}(\mathbf{x}))$ ,  $k_{\mathcal{D}_f}^{\alpha, n}(\mathbf{x}) = k_f^\alpha(\mathbf{x}, S_{\mathcal{D}_f}^{\alpha, n}(\mathbf{x}))$ .

**Convergence analysis:** We present in Theorem 1 below the main theoretical result obtained in [2]. Let  $\rho_T$  denote the insphere diameter of a given tetrahedron  $T$ ,  $h_T$  its diameter, and  $h_{\mathcal{T}} = \max_{T \in \mathcal{T}} h_T$ . We will assume in the convergence analysis that the family of tetrahedral submeshes  $\mathcal{T}$  is shape regular in the sense that  $\theta_{\mathcal{T}} = \max_{T \in \mathcal{T}} \frac{h_T}{\rho_T}$  and  $\gamma_{\mathcal{M}} = \max_{K \in \mathcal{M}} \text{Card}(\mathcal{V}_K)$  are uniformly bounded. The assumptions on the data are natural extensions to our hybrid dimensional model (1) of the assumptions stated in [4]. They are quite general, except for the assumption  $k_m^\alpha(\mathbf{x}, s)$  (resp.  $k_f^\alpha(\mathbf{x}, s)$ )  $\in [k_{\min}, k_{\max}]$  for  $(\mathbf{x}, s) \in \Omega \times [0, 1]$  (resp.  $(\mathbf{x}, s) \in \Gamma \times [0, 1]$ ) which is needed in the following convergence analysis but not in the practical implementation of the scheme. Using the discrete phase pressures as test functions in the discrete variational formulation (2), we deduce the following a priori estimate.

**Lemma 1.** *Let  $u^\alpha$ ,  $\alpha \in \{1, 2\}$ , be a solution to (2), then, there exists  $C > 0$  depending only on the data and on  $\gamma_{\mathcal{M}}$  and  $\theta_{\mathcal{T}}$  such that  $\sum_{\alpha \in \{1, 2\}} \sum_{n=1}^N \Delta t^n \|\pi_{\mathcal{T}} u^{\alpha, n}\|_V^2 \leq C$ .*

Using a topological degree argument, this estimate allows to obtain the existence of a discrete solution to (2). For all  $v = (v^n \in X_{\mathcal{D}, \Delta t})_{n \in \{1, \dots, N\}}$  let us define  $\pi_{\mathcal{D}_m, \Delta t} v(\mathbf{x}, t) = \pi_{\mathcal{D}_m} v^n(\mathbf{x})$ ,  $\pi_{\mathcal{D}_f, \Delta t} v(\mathbf{x}, t) = \pi_{\mathcal{D}_f} v^n(\mathbf{x})$ ,  $\pi_{\mathcal{T}, \Delta t} v(\mathbf{x}, t) = \pi_{\mathcal{T}} v^n(\mathbf{x})$  for all  $(\mathbf{x}, t) \in \Omega \times (t^{n-1}, t^n]$ ,  $n \in \{1, \dots, N\}$ . We also define for  $\alpha \in \{1, 2\}$  the functions  $S_{\mathcal{D}_m, \Delta t}^\alpha(\mathbf{x}, t) = S^\alpha(\mathbf{x}, \pi_{\mathcal{D}_m, \Delta t} p(\mathbf{x}, t))$  and  $S_{\mathcal{D}_f, \Delta t}^\alpha(\mathbf{x}, t) = S^\alpha(\mathbf{x}, \pi_{\mathcal{D}_f, \Delta t} p(\mathbf{x}, t))$ .

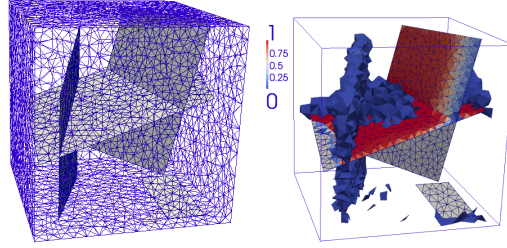
**Theorem 1.** *Let  $(\mathcal{D}^{(k)}, \Delta t^{(k)})_{k \in \mathbb{N}}$  be a sequence of space-time discretizations such that there exist two positive constants  $\theta$  and  $\gamma$  satisfying  $\theta_{\mathcal{T}^{(k)}} \leq \theta$ ,  $\gamma_{\mathcal{M}^{(k)}} \leq \gamma$  for all  $k \in \mathbb{N}$  and such that  $h_{\mathcal{T}^{(k)}}, \max_n \Delta t^{(k), n} \rightarrow 0$  as  $m \rightarrow \infty$ . Let  $u^{\alpha, (k)} \in$*

$X_{\mathcal{D}^{(k)}, \Delta t^{(k)}}, S_{\mathcal{D}_m^{(k)}, \Delta t^{(k)}}^\alpha$  and  $S_{\mathcal{D}_f^{(k)}, \Delta t^{(k)}}^\alpha$ ,  $\alpha \in \{1, 2\}$ , be s.t (2) holds for all  $m \in \mathbb{N}$ . It is also assumed that  $\pi_{\mathcal{D}_m^{(k)}} p^{0, (k)}$  converges strongly to  $p^{\text{ini}}$  in  $L^2(\Omega)$ , and that  $\pi_{\mathcal{D}_f^{(k)}} p^{0, (k)}$  converges strongly to  $\gamma p^{\text{ini}}$  in  $L^2(\Gamma)$ . Then, there exists a weak solution  $(\bar{u}^1, \bar{u}^2)$  with  $\bar{p} = \bar{u}^1 - \bar{u}^2$  to the problem (1) such that for each phase  $\alpha \in \{1, 2\}$  and up to a subsequence, one has  $\pi_{\mathcal{D}^{(k)}, \Delta t^{(k)}} u^{\alpha, (k)} \rightharpoonup \bar{u}^\alpha$  in  $L^2(\Omega \times (0, T))$  and  $\gamma \pi_{\mathcal{D}^{(k)}, \Delta t^{(k)}} u^{\alpha, (k)} \rightharpoonup \gamma \bar{u}^\alpha$  in  $L^2(\Gamma \times (0, T))$ ,  $S_{\mathcal{D}_m^{(k)}, \Delta t^{(k)}}^\alpha \rightarrow S_m^\alpha(\cdot, \bar{p})$  in  $L^2(\Omega \times (0, T))$  and  $S_{\mathcal{D}_f^{(k)}, \Delta t^{(k)}}^\alpha \rightarrow S_f^\alpha(\cdot, \gamma \bar{p})$  in  $L^2(\Gamma \times (0, T))$ .

### 3 Numerical experiments

This test case considers the migration of oil in a 3D basin  $\Omega = (0, L) \times (0, L) \times (0, H)$  with  $H = L = 100$  m. The family of 4 tetrahedral meshes is generated using TetGen [7] in order to be refined at the neighbourhood of the fracture network with a number of cells ranging from 47670 to 3076262 and a factor of refinement at the matrix fracture interface of roughly 12 (see Figure 1 for the coarsest mesh  $i_{\text{mesh}} = 1$ ).

**Fig. 1** Coarsest mesh  $i_{\text{mesh}} = 1$  and discrete solution obtained by the VAG-1 scheme with this mesh at final time: oil saturation in the fracture network and in the matrix using the lower threshold in the matrix equal to 0.001.



The permeability of the matrix  $\Lambda_m = \lambda_m \text{Id}$  and the permeability of the fractures  $\Lambda_f = \lambda_f \text{Id}$  are highly contrasted with  $\lambda_m = 10^{-17} \text{ m}^2$ ,  $\lambda_f = 10^{-11} \text{ m}^2$ . The width of the fractures is fixed to  $d_f = 0.01$  m and their porosity to  $\phi_f = 0.3$ . The porosity of the matrix is set to  $\phi_m = 0.1$ . The inverses of the capillary pressure monotone graph in the matrix ( $j = m$ ) and in the fractures ( $j = f$ ) are defined by the Corey law  $S_j^1(p) = 0$  if  $p < 0$  and  $S_j^1(p) = (1 - s_{r,j}^2)(1 - e^{-\frac{p}{b_j}})$  if  $p \geq 0$  with the rocktype  $b_m = 5 \cdot 10^3$  Pa,  $s_{r,m}^2 = 0.2$ ,  $s_{r,m}^1 = 0$  in the matrix and the rocktype  $b_f = 10^2$  Pa,  $s_{r,f}^2 = s_{r,f}^1 = 0$  in the fractures. The mobilities are defined for  $j = m$  and  $j = f$  by the following Corey law  $k_j^\alpha(\mathbf{x}, s^\alpha) = 0$  if  $\bar{s}^\alpha < 0$ ,  $k_j^\alpha(\mathbf{x}, s^\alpha) = \frac{1}{\mu^\alpha}$  if  $\bar{s}^\alpha > 1$  and  $k_j^\alpha(\mathbf{x}, s^\alpha) = \frac{(\bar{s}^\alpha)^2}{\mu^\alpha}$  if  $\bar{s}^\alpha \in (0, 1)$ , for phase  $\alpha = 1$  (oil), and phase  $\alpha = 2$  (water) where  $\bar{s}^1 = \frac{s^1 - s_{r,j}^1}{1 - s_{r,j}^1 - s_{r,j}^2}$ , and  $\bar{s}^2 = \frac{s^2 - s_{r,j}^2}{1 - s_{r,j}^2 - s_{r,j}^1}$  are the reduced saturations, and  $\mu^1 = 0.005$  Pa.s and  $\mu^2 = 0.001$  Pa.s are the viscosities of the phases. The densities of phases are fixed to  $\rho^1 = 700$  Kg/m<sup>3</sup> for the oil phase and  $\rho^2 = 1000$  Kg/m<sup>3</sup> for the water



phase. Phase 1 is injected at the bottom boundary with imposed pressures  $u^2(\mathbf{x}) = 8.1 \cdot 10^6 + \rho^2 g H$  Pa,  $u^1(\mathbf{x}) = u^2(\mathbf{x}) + (S_f^1)^{-1}(0.999999)$  corresponding to an input phase 1 saturation  $s^1 = 0.999999$  in the fractures. At the top boundary, the phase pressures are fixed to  $u^2(\mathbf{x}) = 8 \cdot 10^6$  and  $u^1(\mathbf{x}) = u^2(\mathbf{x})$ . The remaining boundaries of the basin are assumed to be impervious. The boundaries of the fracture network not located at the top or bottom boundaries of the basin are also assumed impervious. At initial time the porous media is saturated with phase 2 with a hydrostatic pressure  $u_{ini}^2(\mathbf{x}) = 8 \cdot 10^6 + \rho_2 g (H - y)$ , and a phase 1 pressure defined by  $u_{ini}^1(\mathbf{x}) = u_{ini}^2(\mathbf{x})$ .

The implementation of the VAG scheme is based on a flux formulation with up-winding of the mobilities rather than the discrete variational formulation (2) in order to improve the stability of the solution on coarse meshes for convective dominant regimes. The nonlinear systems obtained at each time step are solved by a Newton Raphson algorithm. The time stepping is defined by an initial time step, a maximum time step and the following rule: if the Newton solver does not converge after 20 iterations, the time step is chopped by a factor 2 and recomputed. The time step is increased by a factor 1.2 after each successful time step until it reaches again the maximum time step. The stopping criteria are fixed to  $10^{-7}$  for the GMRes solver and to  $10^{-6}$  for the Newton solver. A CPR-AMG right preconditioner is used in the GMRes iterative solver. Let us also stress that, using the two equations in each cell, the cell unknowns are eliminated from the discrete linearized system at each Newton iteration without any fill-in, reducing the Jacobian system to nodal and fracture face unknowns only. The simulation is run over a period of 10 years with an initial time step of 0.2 days, and a maximum time step fixed to 5 days, except on mesh 4 for which a smaller maximum time step of 2.5 days is used. All the numerical tests have been performed on the Cicada Cluster located at the University Nice Sophia-Antipolis and which includes 1152 nodes equipped with two eight-core Intel(R) E5-2670 processors. Figure 1 exhibits the oil saturation obtained on the coarsest mesh  $i_{mesh} = 1$  at final simulation time. We observe that the oil phase injected at the bottom side in the domain initially saturated with water, quickly rises by gravity along the faults and slowly penetrate in the matrix.

Figure 2 compares the convergence of the oil saturation on the family of refined meshes for two choices of the volume fractions VAG-1 and VAG-2. The choice VAG-2 simply set  $\alpha_{K,s} = \alpha_{K,\sigma} = 0.1$  and  $\alpha_{\sigma,e} = 0.075$  on the whole mesh while the choice VAG-1 does not mix the fracture and matrix porous volume taking  $\alpha_{K,s} = \alpha_{K,\sigma} = 0$  for all  $s \in \mathcal{V}_\Gamma$  and  $\sigma \in \mathcal{F}_\Gamma$ . One can see that, for such high ratio of the fracture and matrix permeabilities, VAG-1 seems to provide a much better convergence than VAG-2 since it does not mix porous volumes from the matrix and the fracture network. This is confirmed by the 2D test case presented in [2] for which a reference solution is computed on a fine grid. It illustrates again the advantage of the VAG scheme compared with CVFE discretizations which cannot avoid such mixing of porous volumes [6], [5]. Table 1 presents the numerical behaviour of the simulations for both choices of the distribution of the volumes and for the family of meshes. The results obtained demonstrate the good robustness and scalability of the proposed numerical scheme both in terms of Newton convergence, linear solver convergence and CPU time.

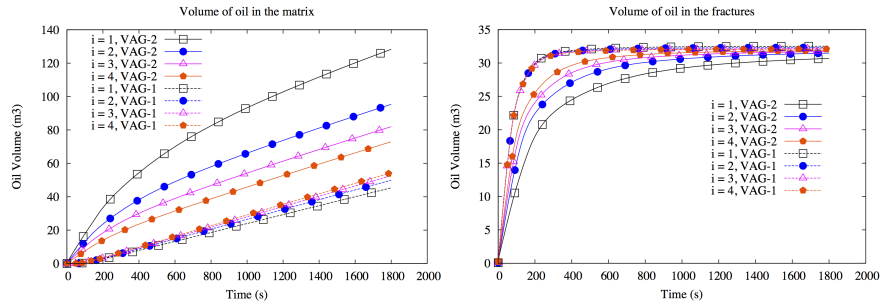


**Fig. 2** Volumes of oil in the fracture and in the matrix function of time for the family of meshes  $i_{mesh} = 1, \dots, 4$ , and for both choices VAG-1 and VAG-2 of the volume distribution.

**Table 1** For each choice VAG-1 and VAG-2 of the volume distribution and for each mesh  $i_{mesh} = 1, \dots, 4$ : number  $N_{\Delta t}$  of successful time steps, number  $N_{Chop}$  of time step chops, number  $N_{Newton}$  of Newton iterations per successful time step, number  $N_{GMRes}$  of GMRes iterations by Newton iteration, CPU time in seconds.

$i_{mesh}$		$N_{\Delta t}$	$N_{Chop}$	$N_{Newton}$	$N_{GMRes}$	CPU (s)		$N_{\Delta t}$	$N_{Chop}$	$N_{Newton}$	$N_{GMRes}$	CPU (s)
1	VAG-1	384	6	2.20	10.05	588	VAG-2	373	0	1.87	6.94	482
2	VAG-1	390	10	3.08	15.11	5 898	VAG-2	373	0	2.42	13.05	4 452
3	VAG-1	415	21	4.02	15.93	31 806	VAG-2	375	1	3.02	14.56	21 645
4	VAG-1	784	30	3.37	16.75	209 485	VAG-2	747	13	2.92	16.55	172 946

**Acknowledgements** The authors would like to thank GDFSuez EP and Storengy for partially supporting this work.

## References

- Alboin, C., Jaffré, J., Roberts, J., Serres, C.: Modeling fractures as interfaces for flow and transport in porous media. Fluid flow and transport in porous media **295**, 13–24 (2002)
- Brenner, K., Groza, M., Guichard, C., Masson, R.: Vertex approximate gradient scheme for hybrid dimensional two-phase darcy flows in fractured porous media. Preprinted, <http://hal.archives-ouvertes.fr/hal-00910939> (2013)
- Eymard, R., Guichard, C., Herbin, R.: Small-stencil 3d schemes for diffusive flows in porous media. ESAIM: M2AN **46**, 265–290 (2010)
- Eymard, R., Guichard, C., Herbin, R., Masson, R.: Gradient schemes for two-phase flow in heterogeneous porous media and Richards equation. ZAMM - Journal of Applied Mathematics and Mechanics (2013). DOI 10.1002/zamm.201200206
- Firoozabadi, A., Monteagudo, J.E.: Control-volume model for simulation of water injection in fractured media: incorporating matrix heterogeneity and reservoir wettability effects. SPE journal **12**, 355–366 (2007)
- Reichenberger, V., Jakobs, H., Bastian, P., Helmig, R.: A mixed-dimensional finite volume method for multiphase flow in fractured porous media. Adv. Water Resources **29**, 1020–1036 (2006)
- Si, H.: TetGen. A quality tetrahedral mesh generator and three-dimensional delaunay triangulator. <http://tetgen.berlios.de> (2007)